Effect of Long-term Aging on Microstructure and Mechanical Properties of 2205 Duplex Stainless Steel at 500℃

Jiawei Wang[1, 2], Xiufang Gong[1, 2], Tianjian Wang[1, 2], Jun Wang[3], Dong Pan[4]

[1]Dongfang Electric Corporation Dongfang Turbine Co., LTD, Deyang 618000, China
[2]State Key Laboratory of Long-Life High Temperature Materials, Deyang 618000, China
[3]School of Material Science and Engineering; Sichuan University, Chengdou 610065, PR China
[4]Nuceal Power Institute of China, Chengdou 610041, China

Abstract. The microstructure and mechanical properties of 2205 duplex stainless steel (DSS) during long-term aging at 500°C were studied. The results showed the hardness of specimens increased all the time during aging, reach the peak with aged for 5800h. Besides, aging at 500°C led to a significant decrease in toughness and notable increase in strength. Fractographs showed that, with increasing aging time, the fracture morphology changed from fibrous fracture to Tran's granular and intragranular fracture. Finally, the changes in microstructure due to aging were studied by optical microscope, scanning electron microscopy and transmission electron microscopy. Transmission electron micrographs revealed that many dislocations and precipitates were distributed along α/γ and α/α interfaces. The precipitates were extracted and confirmed by diffraction pattern to be Cr2N and R-phase; they precipitate from the ferrite phase. Therefore, it can be concluded that dislocation, Cr2N and R-phase are the main reason for the egligible effects on mechanical properties in aged 2205 DSS. The mechanical properties are mainly influenced by the microstructure of ferrite.

1. Introduction

Duplex stainless steel is constituted by a two-phase microstructure with a balance between austenite (γ) and ferrite (α). This structural provide superior properties for the DSS, such as high mechanical resistance, high resistance to stress corrosion, intergranular corrosion and pitting [1-4]. The excellent combination of mechanical properties and corrosion resistance is the main reason for their increasing application in oil, chemical industries and power plants. It's worth noting that DSS is finding increased application as structural material in critical components of nuclear power plants [5, 6]. In nuclear reactors (PWRs and BWRs), cast DSS is commonly used for primary-pressure-boundary components that is vital for safe of the reactors, e.g. primary cooling pipes, elbows, valve bodies, and pump casings [7]. Therefore, it is important to understand the microstructural evolution and mechanical properties at the service temperature. Service temperatures in the new designing power plant applications are about 400~500°C.

A lot of work have been carried out on the microstructural evolution and mechanical properties of 2205 DDS aged in the high temperature, where σ and χ phase are the primary precipitations [8-9], but it is different when aged in the low temperature, so the microstructural evolution and mechanical

Content from this work may be used under the terms of the Creative Commons Attribution 3.0 licence. Any further distribution of this work must maintain attribution to the author(s) and the title of the work, journal citation and DOI.
Published under licence by IOP Publishing Ltd

properties of 2205 DSS at low temperatures has also been extensively studied [10-13]. Fisher et al [10] were the first to suggest embrittlement and hardness were caused by the decomposition of the ferritic phase in a binary iron–chromium alloy to chromium-rich phase (α′) and an iron-rich phase (α) in the temperature range of 280 ~ 500°C; K.L. Weng et al [11] discussed the effect of isothermal treatment (at temperatures ranging between 400 and 500°C) on toughness and hardness of 2205 DSS, they indicated that the locking of dislocations in the modulated structure leads to the severe embrittlement; J.K. Sahu et al [12] carried out the precipitation behavior and the mechanical properties change in DDS, when embrittled at 475°C.

However, this previous research does not care about the aging time, which is less than 5,000h at 500°C. The purpose of the this paper is to investigate the hardening behavior, tensile behavior, impact energy, fracture toughness and characterize microstructural transformations in 2205 DSS aged more than 5, 000h at 500°C. Transmission electron microscopy (TEM), SEM + EDS were used to examine and elucidate the microstructural evolution.

2. Experimental procedure

The chemical composition of 2205 duplex stainless steel is given in Table 1.The initial material was sheet metal hot rolled to 20mm in an L-T (longitudinal–transverse) orientation by Panzhihua and Steel Group Changcheng Special Steel Co.Ltd (China). This sheet was subsequently cutted into specimens with the dimension of 10mm x10mm x10 mm .These specimens were annealed in an oven-type furnace at 1040°C for 40 min and then water quench.

Table 1. Composition of type 2205 duplex stainless steel (wt. %)

Element	C	Cr	Ni	Si	Mo	N	Mn	P	S	Fe
wt.%	0.014	22.8	5.69	0.36	1.48	0.20	1.42	≤0.02	≤0.001	Bal.

The temper treated of alloy sample was held in an oven-type furnace at 500°C for time exceeding 5, 000h and then subjected to microstructure analyses.

Specimens for optical metallography were prepared from the aged specimens and electrolytic ally etched in a Kurami′s etchant solution at 85°C for 5 mins. The specimens for observing surface feature were performed in a Phenom S4800 scanning electron microscope (SEM+EDS) operated at 5 kV. Specimens for transmission electron microscopy (TEM) were also sliced from the aged specimens, thinned to 0.06 ~ 0.08 mm by abrasion on SiC papers and twin-jet electro polished using a mixture of 10% perchloric acid, 20% glycerol, 70% ethanol, in the temperature range of −5 to −10°C and 20V etching potential.

The bulk hardness was measured by using a Vickers hardness tester with a load of 100gf (HV0.1) and Rockwell hardness C tester (with a load of 150 kg), the final hardness number was the average of five hardness points. Charpy impact specimens were machined from the half radius positions of the original rod along the longitudinal direction, in the form of an 11mm x11mm x56mm bar. After the aging treatments, Charpy specimens were machined in the standard 10mm x10mm x55mm dimensions. Charpy impact tests were carried out at room temperature. Fractography of the impact specimens was performed in a Leo 1530 scanning electron microscope (SEM) operated at 15 kV.

3. Result and discussion

3.1. Solution annealing microstructure

Fig. 1 shows the optical micrographs of 2205 DDS after solution annealing treatment (1040°C for 40min, water quenching). In this structure, austenite (γ) phase (etched bright) and ferrite phase (δ) (etched dark) is obvious to be seen, but no other secondary precipitates is found. It is evident that a banded texture of elongated γ islands is observed on the longitudinal section (Fig. 1 (a)), while the more isotropic structure of γ-grain is found on the transverse section (Fig. 1 (b)). The concentration of major alloying elements

in the δ and γ phases for the as-received specimen is analyzed by EDS (Table 2). As expected, δ-ferrite consists higher content of Cr, Mo and Si, while the γ phase contains more Ni and Mn.

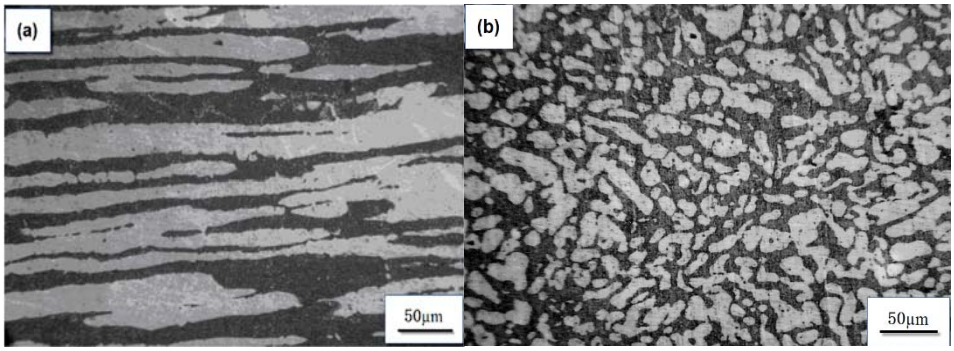

Figure 1. Optical micrographs of soluted steel (1040°C for 40 min): (a) longitudinal section; (b) Transverse section.

Table 2. Chemical composition of the as-received specimen in 2205 DDS by EDS (Atomic %)

Element	Fe	Cr	Ni	Mo	Mn	Si	C
δ	54.47	22.73	3.15	2.04	1.20	0.77	12.62
γ	54.15	17.84	4.79	1.47	1.23	0.72	16.28

3.2. Microstructural evolution during aging

The microstructural evolution during isothermal aging at 500°C is shown in Fig. 2. It is clear that, in as-received material, the structure mainly consists of austenite (γ) within a matrix of ferrite (δ) and no secondary phase is observed at the interface boundaries of γ-δ (Fig. 1). However, the secondary phase particles began to appear, particularly after aging 1 month, and the amount of secondary phases increase with increasing aging time (Fig. 2 (b) and (c)). It is also obvious that secondary phases are precipitated from ferrites, while the microstructure of austenite phases have not changed much all the time. Fig. 2 (d) presents the morphology of precipitates from ferrite phases, the shape of which are columnar, lamellar and showing asteroidal distributions.

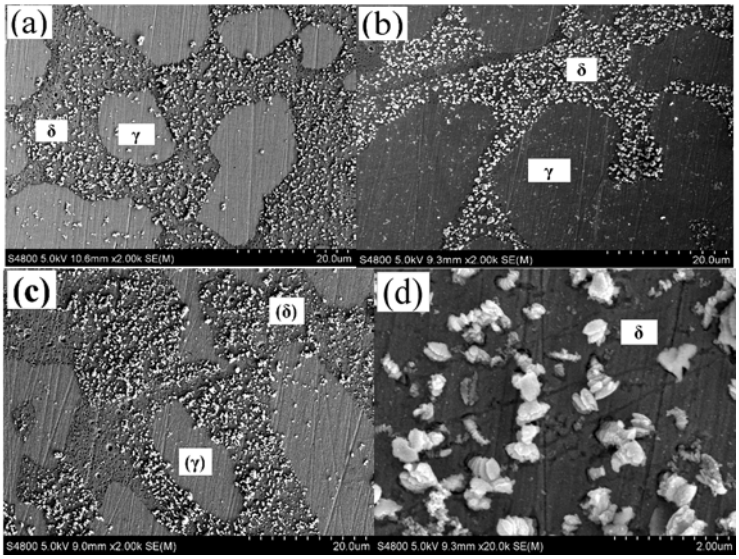

Figure 2. Scanning electron micrographs obtained from 2205 duplex stainless steel aged at 500 °C for: (a) 1450 h; (b) 3600h; (c) 5800h; (d) the partial enlarged drawing of ferrite phases for (c-elliptic area).

Fig. 3 shows the results of TEM of the dislocation structure of the alloy aged at 500°C for different time. After aging for 1450h at 500°C, A lot of dislocations lines are generated in the precipitate-free ferritic region, as shown in Fig. 3a. With the increasing aging time at 500°C, The dimensions of dislocation have become shorter, and the morphology of dislocation changes from lines to loops (Fig. 3 (b) and (c)). From Fig. 3 (d), we can get that the crystalline structure of ferrite phase has changed, which has decomposed into a Cr-rich a phases and Fe-rich α′ phases [14] by nucleation and growth.

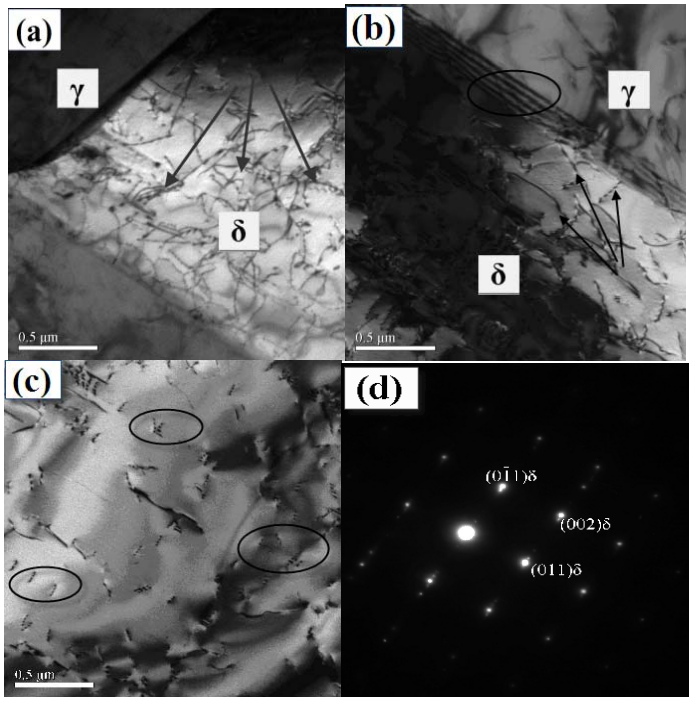

Figure 3. Dislocation structure of 2205 DSS samples aged at 500°C for (a) 1450 h; (b) 3600h; (c) 5800h; (d) SADP diffraction pattern with [1 0 0] zone axis.

Previous work has been carried out that [15], the precipitates of Cr2N occurs as a shap of fine needle from grain boundaries of γ-δ (Fig.4 (a) [black arrowed]) after aging for 1450h at 500°C, with a size of about 120 nm in the long axis. Wilms [16] and Shi [17] discussed that the nucleation and growth of Cr2N precipitates were governed by the diffusion of Cr atoms and N atoms. Nucleation of this phase is highly favored by the extra energy associated with dislocations. Small fine needle particles of chromium nitride (Cr2N) (Fig. 4(b) [black arrowed]) are grown when the alloy aging for 3600h at 500°C. After aging for 5800h at 500°C, the needle-shape chromium nitrides (Cr2N) (Fig. 4 (c), black arrowed) generated not only on the grain boundaries of γ-δ, but also in ferrite phase. And the sizes of Cr2N have grown to 500–650 nm in the long axis.

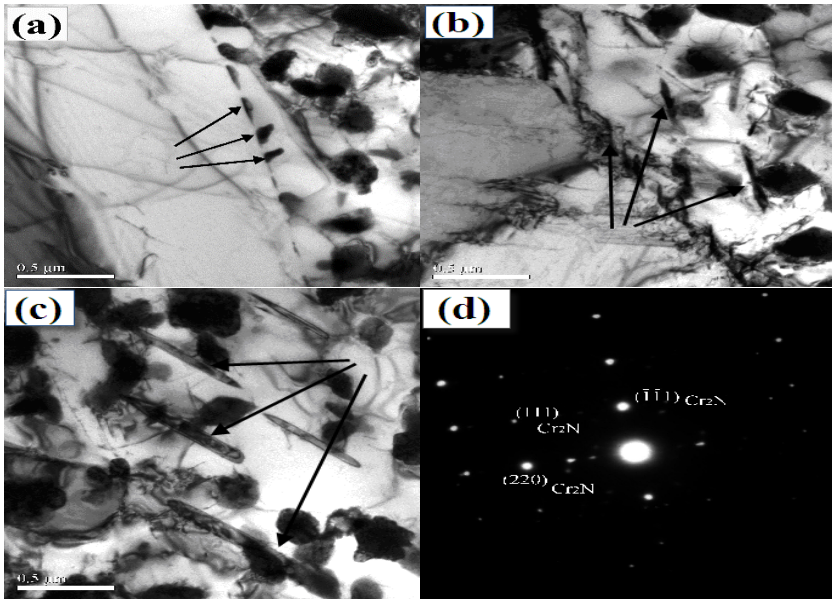

Figure 4. Cr_2N precipitates of 2205 DSS samples aged at 500°C for (a) 1450 h; (b) 3600h; (c) 5800h; (d) SADP of (a) with [1 1 2] zone axis.

Fig. 5 (a) shows a new precipitate was generated in ferrite phases after the alloy aging for 3600h at 500°C. By using the SADP (Fig. 5 (c), it can be seen that the new precipitation identified in the alloy is R-phase (Fe2Mo), which are irregular granular on the surface of ferrite phase. As shown in Fig. 5 (b), with the increasing of aging time, the R phase has grown to be globular, and the size of it has become larger.

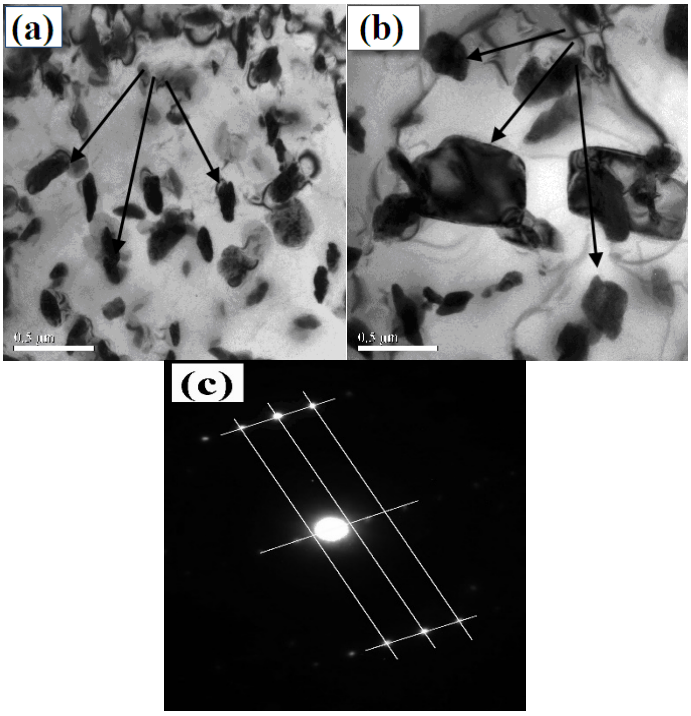

Figure 5. R-phases of 2205 DSS samples aged at 500 °C for (a) 3600h; (b) 5800h; (c) SADP of (b) with [$\bar{2}$ 5 2] zone axis

3.3. Effect of aging on micro hardness

Fig. 6 shows the variation of Rockwell C hardness (HRC) as a function of aging time at 500◦C; it indicates that the hardness increases with increasing aging time. Obviously, at tested ageing temperature ,the increase rate of hardness is quite high at the beginning 1 month of aging .From then on , the increase in hardness is slow down relativity, after aging 5 months, the hardness reaches its peak value, and then decrease with increasing aging time. Fig. 7 shows the Vickers micro-hardness of 2205 DDS aged at 500 ◦C for different aging time; it can see that, the hardness of δ-ferrite change with aging times, while the hardness of austenite appears to be nearly the same. The changing trend of the hardness of δ-ferrite corresponds to the matrix. Therefore, the hardness in the steel is mainly associated with the aging hardening of δ-ferrite, similar to the results reported by K.L. Weng [11].

This result suggests that the hardness of DSS is presumably connected with the microstructural evolution of δ-ferrite. For the first month of aging, because of the high density of dislocation in the precipitate-free ferritic (Fig.8 (c).), it will make an effect on redistribution of atoms, therefore, it will predominantly increase the hardness of ferrite phase [18-20]. At the fifth month, the precipitation of R-phase in ferrite phase is a high hardness intermetallic, which may cause hardness greatly increased. However, the precipitation of Cr2N (Fig. 10) leads to decrease in hardness of ferrite phase. At eariler stage, its effect is not obviously, with the increasing aging time, it grows up. Meanwhile, the dislocation reduces the effect on the hardness of ferrite, due to size decreases. So the Cr2N plays dominant role in decline of hardness at last.

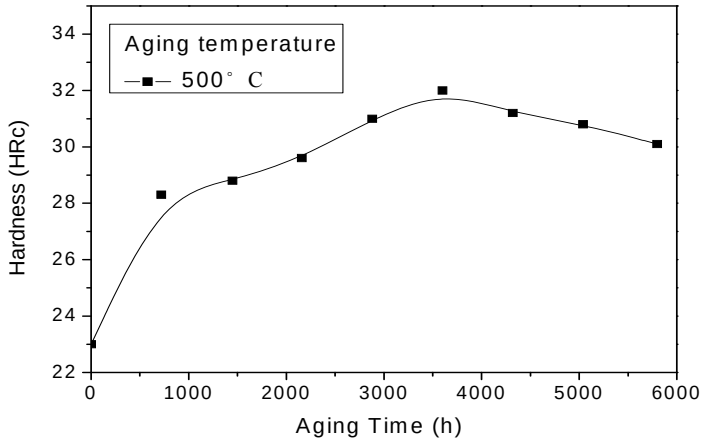

Figure 6. Effect of aging treatments on HRC micro-hardness of 2205 stainless steel for the aging temperatures 500°C.

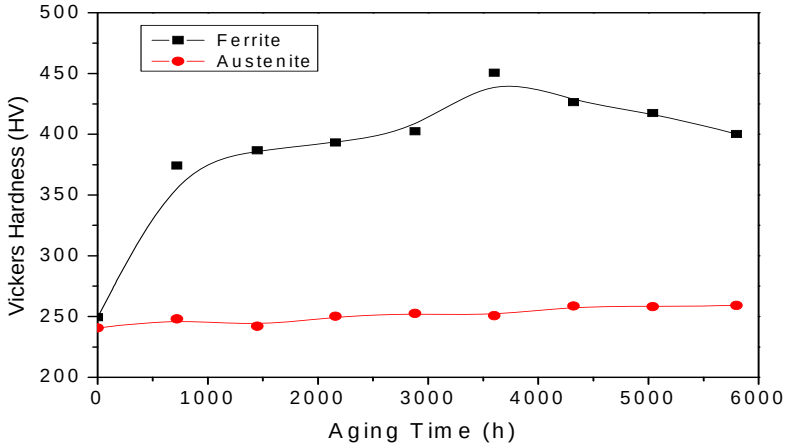

Figure 7. Vickers micro-hardness of δ-ferrite and austenite for the aging temperatures 500°C.

3.4. Effect of aging on tensile behaviour

Fig. 8 shows the strength of 2205 DDS aged at 500°C for different aging time, it can be seen that the strength, including tensile stress (σUTS) and yield stress (σYS), increases obviously with increasing aging time at 500°C. In the initial stage, strength rises fast, then slows down after aging for 3 month.

The dislocation lines are generated in ferrite phase with the aging, and interact with the particles. The particles hinder the dislocation motion, dislocation then piles up on the suface, and makes it difficult to move. Due to the generation of dislocation and precipitation, they improve the ability of material deformation and increase strength of the 2205 DDS. However, the precipitation of Cr2N leads to poor chromium in the matrix and grain boundaries, it decreases the strength, impact toughness and corrosion resistance obviously. So the increase rate of strength slows down after aging for 4 month.

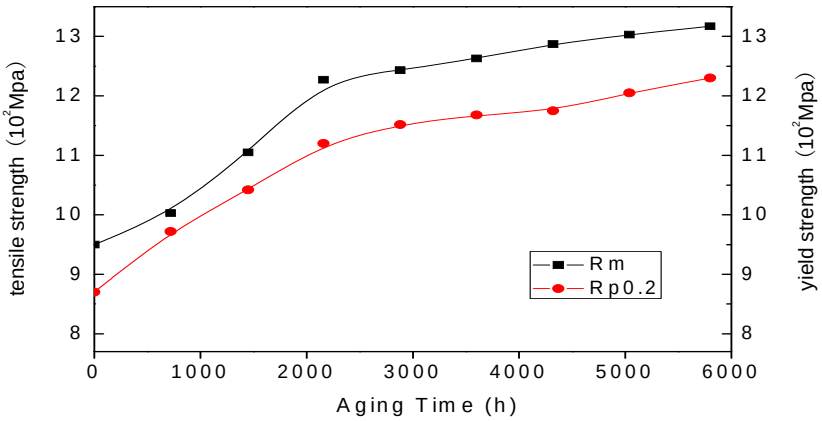

Figure 8. Tensile change of 2205 stainless steel in long term aging at 500°C.

3.5. Effect of aging on charpy impact toughness

Fig. 9 shows the absorbed energy before fracture of 2205 DDS aged 500°C for different aging time, it can be seen that the absorbed energy decreases with increasing aging time. At the beginning of 1month, the impact energy is just 32 J, when compared with the specimens without aging (i.e., the impact energy of the as-received material is 304 J [11]). After aging at 500°C for 8 month, the impact energy decreases to 18 J. It is evident that aging at 500°C for a long time leads to severe deterioration in the toughness of the steel.

The dislocation lines interact with the precipitation can decrease the impact energy. It provides strong support to suggest that the immobilization of dislocations in δ-ferrite is detrimental to toughness. With increasing aging time, more Cr2N particles are precipitated at phase interfaces and grain boundaries, causing the continuous decrease of impact energy [21]. So the impact energy decreased all the time during the aging.

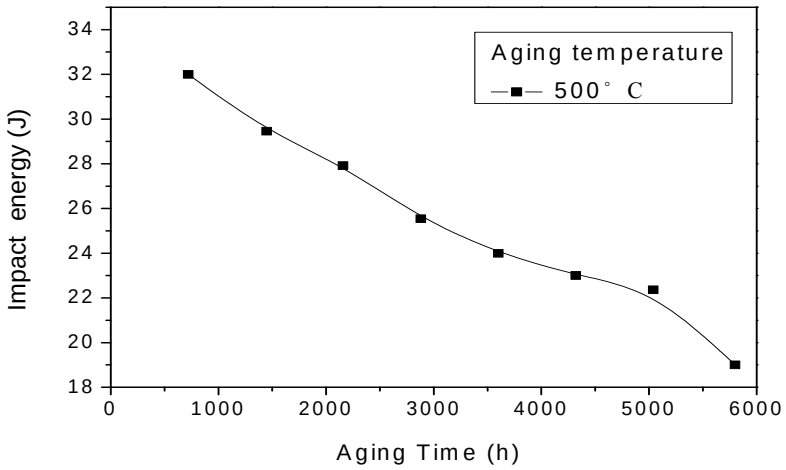

Figure 9. Effect of aging treatments on Charpy V impact energy of 2205 DDS aged at 500°C

3.6. Effect of aging on charpy impact fracture morphologies

Fig.10 show the fracture surfaces of Charpy impact specimens aged at 500°C for different aging times. It is evident that the fracture surfaces of as-received material consisted a large number of deep dimples as shown in Fig. 10 (a). After an aging time of 2 month, the fracture appearance (Fig. 10 (b)) appears small and poorly facets, the dimples become shallow and the amount of dimples decrease obviously. In the specimen aged at 500°C for 5 months (Fig. 10 (c)), a typical tear ridges can be observed. After aged at 500°C for 8 months, the fracture (Fig. 10 (d)) shows cleavage-like areas, this reveals that brittle fracture mechanism has become dominant.

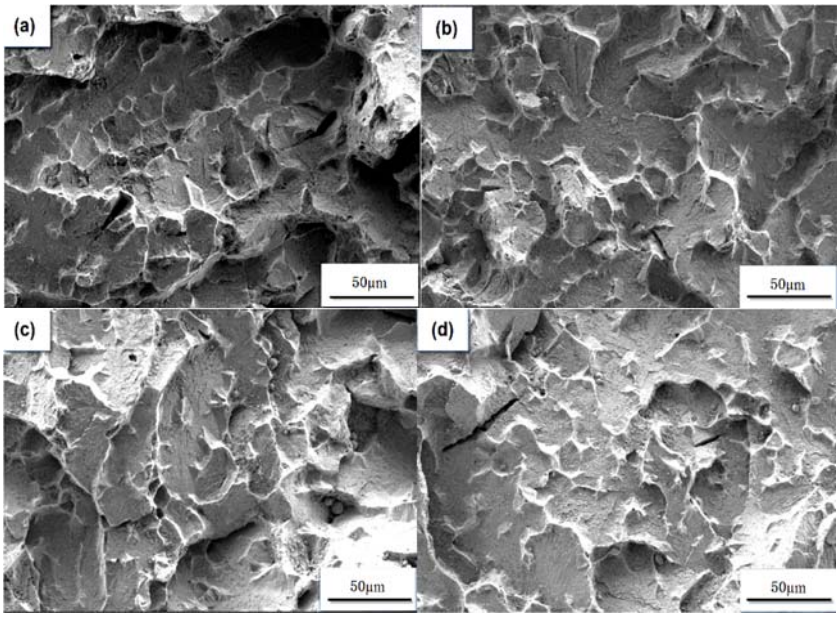

Figure 10. Fractograph after impact testing of 2205 duplex stainless steel aged at 500°C for (a) as-received; (b) 1450 h; (c) 3600h; (d) 5800h;

4. Conclusion

The effects of aging treatment at the temperature of 500°C for 0-5800h on the microstructures and consequent mechanical properties of a 2205 duplex stainless steel have been investigated. The important findings are summarized as follows.

The evidence shows that the dislocation lines are generated in the δ-ferrite, became shorter and shorter during the aging, and the dislocation loops are formed after aged 5800h due to interact with the precipitations. The Cr-rich Cr2N particles are precipitated from δ-ferrite, clustering and growing during the aging. However, the intermetallic R-phase precipitated at the interface of δ/γ in the specimen aged at 500°C after 3600h. That the R-phase grew into spherical with the clustering.

With the discussion before, the microstructural evolution during aging at 500°C have great effect on the mechanical properties, including hardness, tensile behavior and impact toughness. The embrittlement phenomenon is accompanied by an increase in hardness, tensile behavior and impact toughness.

This result suggests that the embrittlement phenomenon of the duplex stainless steel studied is presumably connected with the microstructural evolution of δ-ferrite.

References

[1] Michalska J, Sozanska M. Qualitative and quantitative analysis of σ and χ phases in 2205 duplex stainless steel. Mater Charact 2006; 56: 355 – 62.
[2] Nilsson JO. Super duplex stainless steels. Mater Sci Technol 1992; 8: 685–700.
[3] Tan Hua, Jiang Yiming, Deng Bo, Sun Tao, Xu Juliang, Li Jin. Effect of annealing temperature on the pitting corrosion resistance of super duplex stainless steel UNS S32750. Mater Charact 2009; 60: 1049 – 54.
[4] Perren RA, Suter T. Corrosion resistance of super duplex stainless steels in chloride ion containing environments:investigations by means a new microelectrochemical method: II. Influence of precipitates. Corros Sci 2001; 43: 727 – 45.
[5] Cheon JS, Kim IS. Evaluation of thermal aging embrittlement in CF8 duplex stainless steel by small punch test. Journal of Nuclear Materials 2000; 278: 96 – 103.
[6] Kwon JD, Woo SW, Lee YS, Park J, Park JC, Park YW. Effects of thermal aging on the low cycle fatigue behavior of austenitic–ferritic duplex cast stainless steel. Nuclear Engineering and Design. 2001; 206: 35 – 44.
[7] Wang Jun, Zou Hong, Wu Xiao-yon, Li Cong, Qiu Shao-yu, Shen Bao-luo. The effect of microstructural evolution on hardening behavior of type 17-4PH stainless steel in long-term aging at 350°C. Mater Charact 2006; 57: 274 – 80.
[8] T.H. Chen, K.L. Weng, J.R. Yang, Mater. Sci. Eng. A338 (2002) 259 – 270.
[9] Joanna Michalska, Maria Sozańska. Qualitative and quantitative analysis of σ and χ phases in 2205 duplex stainless steel. Materials Characterization.56 (2006) 355–362.
[10] Fisher RM, Dulis EJ, Carroll KG. Identification of the precipitate accompanying 885 °F embrittlement in chromium steels. Transactions AIME 1953; 197: 690 – 95.
[11] Weng KL, Chen HR, Yang JR. The low-temperature aging embrittlement in a 2205 duplex stainless steel. Mater Sci Eng A 2004; 379:119–32.
[12] J.K. Sahua, b,∗, U. Kruppc, R.N. Ghosha, H.-J. Christb. Effect of 475◦C embrittlement on the mechanical properties of duplex stainless steel. Materials Science and Engineering A 508 (2009) 1 – 14.
[13] Duprez L, Cooman BD, Akdut N. Microstructure evolution during isothermal annealing of a standard duplex stainless steel type 1.4462. Steel Res 2000; 71:417 – 22.
[14] Shu-kun Shi, Yu Zhang, Jun Wang. The microstructure evolution of 2205 stainless steel in long-term aging at 500◦C. Nuclear Engineering and Design xxx (2012) xxx– xxx.
[15] Sieurin H, Sandstrom R, Westin EM. Fracture toughness of the lean duplex stainless steel LDX 2101. Metall Mater Trans A 2006; 37: 2975 – 81.
[16] Zhang Wei, Jiang Laizhu, Hu Jincheng, Song Hongmei. Effect of ageing on precipitation and impact energy of 2101 economical duplex stainless steel. Mater Charact 2009; 60: 50 – 5.
[17] Llanes L, Mateo A, Iturgoyen L, Anglada M. Aging effects on the cyclic deformation mechanisms of a duplex stainless steel. Acta Materialia 1996; 44: 3967–78.
[18] Horvath W, Prantl W, Stroißnigg H, Werner EA. Microhardness and microstructure of austenite

and ferrite in nitrogen alloyed duplex steels between 20 and 500°C. Mater Sci Eng A 1998; 256: 227 – 36.

[19] Liljas M, Johansson P, Liu H-P, Olsson C-O A. Development of a lean duplex stainless steel. Steel Res Int 2008; 79: 466 – 73.

[20] Effect of Ageing On Precipitation and Impact Energy of 2101 Economical Duplex Stainless Steel [J]. Materials Characterization, 2009, 60: 50.